Peak profiles of the Okorokov effects for heavy ions in a crystal

Y. Yamashita and Y. H. Ohtsuki
Department of Physics, Waseda University, Ohkubo 3, Shinjuku Tokyo 160, Japan
(Received 8 February 1980)

Detailed peak profiles of resonant excitation probabilities of a heavy ion along the crystal axis are calculated taking into account energy-level shifts, splitting of electron states in the heavy ion, and dwell-time differences for different channeling paths. The temperature effect is also studied by calculation of the Debye-Waller factor. The shape of peak profiles calculated for $N^{6+} \rightarrow$ Au $\langle 111 \rangle$ agrees well with the experimental results obtained by Moak *et al.* However, quantitatively, few differences are found for the higher Miller indices.

I. INTRODUCTION

Recently, Moak *et al.*[1] observed the Okorokov effect[2] for heavy ions (N^{6+} ions) into Au $\langle 111 \rangle$, in which the detailed peak profiles of the resonant coherent-excitation probability was given as a function of the ion velocity. The peak profile has a special asymmetrical shape, and the peak width is very large.

Here, making use of our previous theory,[3] we perform detailed calculations of peak profiles of the Okorokov effect, taking into account energy-level shifts and splitting of electron states in the heavy ions, dwell-time differences for different channeling paths, and lattice vibrations.

In Sec. II, we give a general formulation for the probability function of the resonant coherent excitations. We perform the detailed calculation of the matrix element and the probability function over the channeling path in space and time in Sec. III. Numerical results and comparison with experiments are shown in Sec. IV.

II. GENERAL FORMULATION

When the ion moves along the atomic row of the crystal, it experiences the perturbation of the periodic Coulomb potential with the crystal lattice. The angular frequency of the perturbation is $2\pi v/d$, where v is the ion velocity and d the lattice constant. We use $\vec{b}$ for the position of the ion in the section of the axial channel and $\vec{r}$ for the coordinate of the electron as measured from the ion center. The coordinate of the ion is represented by (see Fig. 1)

$$\vec{R}_0(t) = \vec{b} + \vec{v}t, \quad \vec{b} \perp \vec{v} \ , \tag{1}$$

and the coordinate of the electron by

$$\vec{R}(t) = \vec{R}_0(t) + \vec{r} \ . \tag{2}$$

We expand the perturbation potential for the ion in Fourier series with components for the axial direction of the reciprocal-lattice vector, $g_z = m/d$ (m an integer),

$$V(t) = V(\vec{R}(t)) = V(\vec{b}, \vec{v}, \vec{r}, t)$$
$$= i\hbar \sum_m F^{(m)}(\vec{b}, \vec{r}) \exp\left(-i\frac{2\pi m v}{d}t\right) \ , \tag{3}$$

where

$$F^{(m)}(\vec{b}, \vec{r}) = \frac{1}{i\hbar} \sum_{g_\perp} V_{g_\perp, m/d} \exp(-i2\pi \vec{g} \cdot \vec{b})$$
$$\times \exp(-i2\pi \vec{g}_\perp \cdot \vec{r}_\perp - i2\pi m z/d) \ . \tag{4}$$

We insert the perturbed Hamiltonian V in the Schrödinger equation, and expand the wave function Ψ with the eigenfunction of the unperturbed Hamiltonian H_0,

$$i\hbar \frac{\partial \Psi}{\partial t} = (H_0 + V)\Psi \ , \tag{5}$$

$$\Psi(t) = \sum_k A_k(t)\psi_k \exp(-iE_k t/\hbar) \ , \tag{6}$$

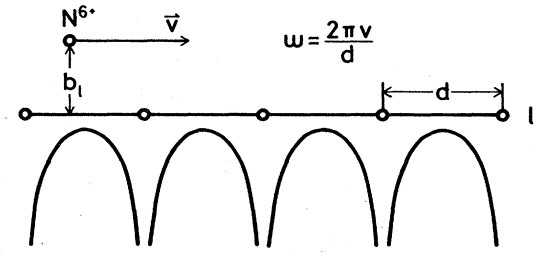

FIG. 1. The ion moving in the periodic Coulomb fields (the subscript l means the number of the string, and b_l the impact parameter for the string).

where $H_0\psi_k = E_k\psi_k$, from which we obtain

$$\frac{d}{dt}A_n(t) = \sum_k \sum_m F_{nk}^{(m)}(\vec{b}) \exp(i\epsilon_{nk}^{(m)}t) A_k(t) \quad , \tag{7}$$

where $F_{nk}^{(m)}$ is the matrix element of Eq. (4) and

$$\epsilon_{nk}^{(m)} = \frac{E_n - E_k}{\hbar} - \frac{2\pi m v}{d} \quad . \tag{8}$$

The resonance condition means that

$$\epsilon_{nk}^{(m)} = 0, \quad \frac{E_n - E_k}{\hbar} = \frac{2\pi m v}{d} \quad . \tag{8'}$$

Here we take into account the excitation between the ground state and the first excited states only. When the ion velocity is close to the resonance velocity, the cross terms of these two states mainly contributes to the time integral of Eq. (7) for $m \neq 0$ and the cross terms of degenerate states (including the same states) contribute for $m = 0$, but the contribution from the other terms is small.

We represent the ground state with $n = 0$ and four degenerate first excited states, $2p_z (m_q = 0, m_q$ being the magnetic quantum number), $2s$, $2p_1 (m_q = 1)$, and $2p_{-1} (m_q = -1)$, with $n = 1$–4, respectively. Then we may obtain the set of the differential equations

$$\begin{aligned} \frac{d}{dt}A_0 &= -\sum_{n=1}^{4} F_{n0}^{(m)*} \exp(-i\epsilon_{n0}^{(m)}t) A_n + F_{00}^{(0)} A_0 \quad , \\ \frac{d}{dt}A_n &= F_{n0}^{(m)} \exp(i\epsilon_{n0}^{(m)}t) A_0 \\ &\quad + \sum_{k=1}^{4} F_{kn}^{(0)} A_n \quad (n = 1\text{–}4) \quad , \end{aligned} \tag{9}$$

where $V^{(0)} = i\hbar F^{(0)}$ [$V^{(0)}$ is the average potential or the continuum potential] and $\epsilon_{10}^{(m)} = \epsilon_{20}^{(m)} = \epsilon_{30}^{(m)} = \epsilon_{40}^{(m)} = \epsilon^{(m)}$.

The diagonal terms of the matrix elements of $F^{(0)}$ are not zero, and also the nondiagonal terms of $2s$, $2p_1$, and $2p_{-1}$ are not zero. Therefore we diagonalize them, and we represent the states with n in which the matrix elements of $F^{(0)}$ are diagonalized. Then the first-order differential equations which we have to solve are

$$\begin{aligned} \frac{d}{dt}A_0 &= -\sum_{n=1}^{4} F_{n0}^{(m)*} \exp(-i\epsilon^{(m)}t) A_n + F_{00}^{(0)} A_0 \quad , \\ \frac{d}{dt}A_n &= F_{no}^{(m)} \exp(i\epsilon^{(m)}t) A_0 + F_{nn}^{(0)} A_n \quad (n = 1\text{–}4) \quad . \end{aligned} \tag{10}$$

It is difficult to solve this equation exactly. Here we take the two-states approximation in which the ground state and the single excited state are considered. We obtain

$$|A_n(t)|^2 = \frac{4|F_{n0}^{(m)}|^2}{[\epsilon^{(m)} + (V_{nn}^{(0)} - V_{00}^{(0)})/\hbar]^2 + 4|F_{n0}^{(m)}|^2} \sin^2\left(\frac{1}{2}\{[\epsilon^{(m)} + (V_{nn}^{(0)} - V_{00}^{(0)})/\hbar]^2 + 4|F_{n0}^{(m)}|^2\}^{1/2} t\right) \quad . \tag{11}$$

where $V_{nn}^{(0)}$ is the first-order correction of the eigenenergy of the nth state.

From Eq. (11), the resonance condition [Eq. (8')] may be modified by

$$[(E_n + V_{nn}^{(0)}) - (E_0 + V_{00}^{(0)})]/\hbar = 2\pi m v/d \quad . \tag{12}$$

As mentioned above, the resonance condition is not Eq. (8) but Eq. (12), which depends on $\vec{b}$ and each excited sate.

III. CALCULATION OF THE MATRIX ELEMENT

Because the extent of the wave function is small for the ground and the first excited states, i.e.,

$$\vec{g}\cdot\vec{r} < 1 \quad ,$$

we may approximate

$$\exp(-i2\pi\vec{g}\cdot\vec{r}) \cong 1 - i2\pi g_x x - i2\pi g_y y - i2\pi(m/d)z + \frac{1}{2}(-i2\pi g_x)^2 x^2 + \frac{1}{2}(-i2\pi g_y y)^2 + \frac{1}{2}(-i2\pi m/d)^2 z^2 \quad .$$

Inserting this into Eq. (4), we obtain

$$F^{(m)}(\vec{b}, \vec{r}) \simeq \frac{1}{i\hbar}\left[1 + x\frac{\partial}{\partial b_x} + y\frac{\partial}{\partial b_y} - i2\pi\frac{m}{d}z + \frac{1}{2}x^2\frac{\partial^2}{\partial b_x^2} + \frac{1}{2}y^2\frac{\partial^2}{\partial b_y^2} - 2\pi^2\left[\frac{m}{d}\right]^2 z^2\right] V_{m/d}(\vec{b}) \quad . \tag{13}$$

We take the Moliere potential as the interaction potential between the electron and the individual atoms in the solid, i.e.,

$$V_a(r) = -\frac{Z_2 e^2}{r}\sum_{i=1}^{3}\alpha_i \exp\left[-\frac{\beta_i r}{a_{\mathrm{TF}}}\right] \quad , \tag{14}$$

where $\{\alpha_i\}=\{0.35, 0.55, 0.10\}$, $\{\beta_i\}=\{0.30, 1.20, 6.00\}$, and Z_2 and $a_{\rm TF}$ are the atomic number of the solid and Thomas-Fermi screening length, respectively.

Then we may calculate the potential $V_{m/d}(\vec{b})$ in Eq. (13)

$$V_{m/d}(\vec{b})=\frac{1}{d}\sum_l e^{i2\pi(m/d)\delta_l d}\int_{-\infty}^{\infty}V_a((b_l^2+z^2)^{1/2})e^{i2\pi(m/d)z}=-\frac{2Z_2e^2}{d}\sum_l e^{i2\pi m\delta_l}\sum_{i=1}^{3}\alpha_i K_0\left(b_l\left[\left(\frac{\beta_i}{a_{\rm TF}}\right)^2+\left(\frac{2\pi m}{d}\right)^2\right]^{1/2}\right) , \tag{15}$$

where K_0 is the zero-order modified Bessel function of the second kind, and $\delta_l d$ is the deviation of the lth atomic row to the 1st atomic row for the axial direction (see Fig. 2).

First we will calculate the matrix elements between $1s$, $2p_z$, $2s$, $2p_1(m_q=1)$, and $2p_{-1}(m_q=-1)$. Calculations are not so complicated but are long-winded. So here we show only two matrix elements as an example.

$$F^{(m)}_{2p_i,1s}(\vec{b})=-\frac{i}{\hbar}\left(-\frac{2Z_2e^2}{d}\right)\sum_l e^{i2\pi m\delta_l}\left(\frac{b_{lx}-ib_{ly}}{b_l}\right)$$
$$\times\sum_i\alpha_i\left[\left(\frac{2\pi m}{d}\right)^2+\left(\frac{\beta_i}{a_{\rm TF}}\right)^2\right]^{1/2}\left\{-K_1\left(b_l\left[\left(\frac{2\pi m}{d}\right)^2+\left(\frac{\beta_i}{a_{\rm TF}}\right)^2\right]^{1/2}\right)\right\}\left[-4\left(\frac{2}{3}\right)^5\left(\frac{a_0}{Z_1}\right)\right] , \tag{16}$$

$$V^{(0)}_{1s,1s}(\vec{b})=\left(-\frac{2Z_2e^2}{d}\right)\sum_l\sum_i\left[K_0\left(\frac{\beta_i b_l}{a_{\rm TF}}\right)+\left\{-\frac{1}{b_l}\frac{\beta_i}{a_{\rm TF}}K_1\left(\frac{\beta_i}{a_{\rm TF}}b_l\right)+\frac{1}{2}\left(\frac{\beta_i}{a_{\rm TF}}\right)^2\left[K_0\left(\frac{\beta_i}{a_{\rm TF}}b_l\right)+K_2\left(\frac{\beta_i}{a_{\rm TF}}b_l\right)\right]\right\}\left(\frac{a_0}{Z_1}\right)^2\right] . \tag{17}$$

By the way, we note that

$$F^{(m)}_{2p_{-1},1s}(\vec{b})=-F^{(m)*}_{2p_1,1s}(\vec{b}) , \tag{18}$$

$$V^{(0)}_{2p_{-1},2p_{-1}}(\vec{b})=V^{(0)}_{2p_1,2p_1}(\vec{b}) , \tag{19}$$

$$V^{(0)}_{2p_z,2s}(\vec{b})=V^{(0)}_{2p_z,2p_1}(\vec{b})=V^{(0)}_{2p_z,2p_{-1}}=0 , \tag{20}$$

$$V^{(0)}_{2s,2p_{-1}}(\vec{b})=-V^{(0)*}_{2s,2p_1}(\vec{b}) . \tag{21}$$

Now we represent $1s$, $2p_z$, $2s$, $2p_1$, and $2p_{-1}$ by $n=0$–4, respectively. The matrix formed by the matrix elements of $V^{(0)}$ can be diagonalized by diagonalization of the partial matrix with $2s$, $2p_1$, and $2p_{-1}$, and we can obtain the first-order correction of the eigenvalue of the energy. If the matrix $[V^{(0)}]$ could be diagonalized with the transform matrix S [diagonalized matrix is $S^{-1}(V^{(0)})S$], the basis set of the matrix or the eigenstates of the energy is

$$(\psi_0\psi_1,\psi_2,\psi_3,\psi_4,)^t=S^t(\psi_0\psi_1\psi_2\psi_3\psi_4)^t ,$$
$$\psi_{n'}=\sum_{n=2}^{4}S_{nn'}\psi_n \quad (n'=2,3,4) . \tag{22}$$

Therefore,

$$F^{(m)}_{n'0}=\sum_{n=2}^{4}S^*_{nn'}F^{(m)}_{n0}, \quad (n'=2,3,4) . \tag{23}$$

Hereafter we omit the prime indication for simplicity.

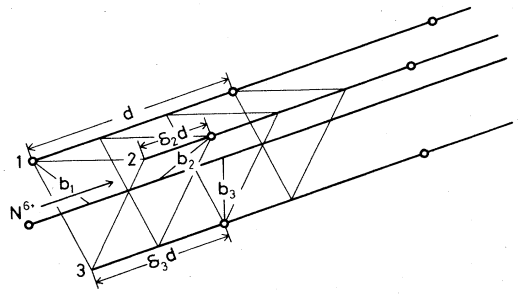

FIG. 2. The ion moving in the axial channel. b_l is the impact parameter from the lth string, and $\delta_l d$ is the deviation of it to the 1st string for the axial direction.

IV. RELATION TO THE EXPERIMENTAL

Moak *et al.*[1] observed the rate of the ions which were not ionized (survival fraction) after the passing through the crystal with various velocity, considering the fact that the ion can be easily ionized when it is in excited states. In Fig. 3, the experimental result[1] is shown for the ionization probability from N^{6+} to N^{7+} by the electron impact in the solid. At the top of the figure, we show the subtraction of the survival fraction from the background.

Now we calculate the ionization probability on the assumption that only the ionization channel, where the ion is excited by Okorokov effect and the excited ion is ionized by electron impact in the solid, exists. We denote subscript "old" when we ignore the ionization process, and subscript "new" when we consider

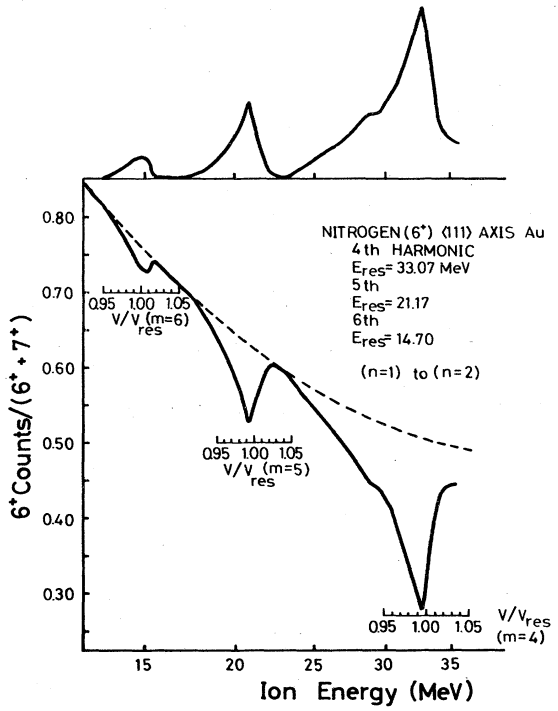

FIG. 3. Experimental ionization probability of N^{6+} ions into Au ⟨111⟩ by Moak *et al.* (Ref. 1).

the ioinization process. We denote subscript "∞" for ionized states. The probability conservation shows that

$$|A_0(t)|^2_{\text{old}} + \sum_{n=1}^{4} |A_n(t)|^2_{\text{old}} = 1 \ , \tag{24}$$

$$|A_0(t)|^2_{\text{new}} + \sum_{n=1}^{4} |A_n(t)|^2_{\text{new}} = 1 - |A_\infty(t)|^2 \ . \tag{25}$$

Here we note that the ratio of the occupation weight for every discrete level is not changed when we consider the ionization process. Thus we obtain

$$|A_n(t)|^2_{\text{new}} = |A_n(t)|^2_{\text{old}} (1 - |A_\infty(t)|^2) \tag{26}$$

and the time differential coefficient of the ionization transition probability $|A_\infty(t)|^2$ is calculated by

$$\frac{d}{dt}|A_\infty(t)|^2 = \sum_{n=1}^{4} N v \sigma_{n\infty} |A_n(t)|^2_{\text{new}}$$

$$= \sum_{n=1}^{4} N v \sigma_{n\infty} |A_n(t)|^2_{\text{old}} (1 - |A_\infty(t)|^2) \ , \tag{27}$$

where N is the density of the electron which contributes to the ionization of an ion by the impact, and $\sigma_{n\infty}$ the ionization cross section. The time integral of Eq. (27) gives the ionization probability

$$|A_\infty(t_0)|^2 = 1 - \exp\left[- \sum_{n=1}^{4} N \sigma_{n\infty} D P_n(t_0) \right] \ ,$$

$$P_n(t_0) = \frac{1}{t_0} \int_0^{t_0} |A_n(t)|^2_{\text{old}} \, dt \ , \tag{28}$$

where D is the thickness of the target and t_0 the dwell time through the crystal. In the above, $P_n(t_0)$ means the averaged excitation probability by the Okorokov effect.

V. CHANNELING AVERAGE AND PEAK PROFILE

Finally we make an average of the excitation probability for the channeling path. We do this with the statistical-equilibrium spatial distribution (SESD) of the ion path for the parallel incidence and the perfect alignment.

In Fig. 4 we show Au ⟨111⟩ axial channel. We make the channeling average only for the shadowed region in the Fig. 4 because the other regions are identical.

The first-order corrections of the eigenenergies for the four first excited states $[V^{(0)}_{nn} - V^{(0)}_{00}$ (for $n = 1-4)]$ were calculated in detail. We show our results for $V^{(0)}_{nn} - V^{(0)}_{00}$ in Fig. 5. The solid curve indicates the changes of these quantities from O to C and the dashed curve the changes along the $O - X$ direction in Fig. 4.

In Fig. 6, we show the averaged excitation probabilities, $\langle Pn \rangle_{\text{channel}}$, for each excitation level (1–4) in the case of $N^{6+} \rightarrow$ Au ⟨111⟩ ($m = 4,6$). v_{res} means

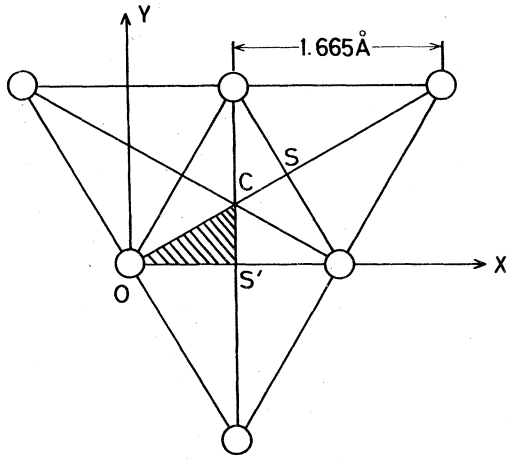

FIG. 4. Au ⟨111⟩ axial channel. The shadowed region is a symmetrical one.

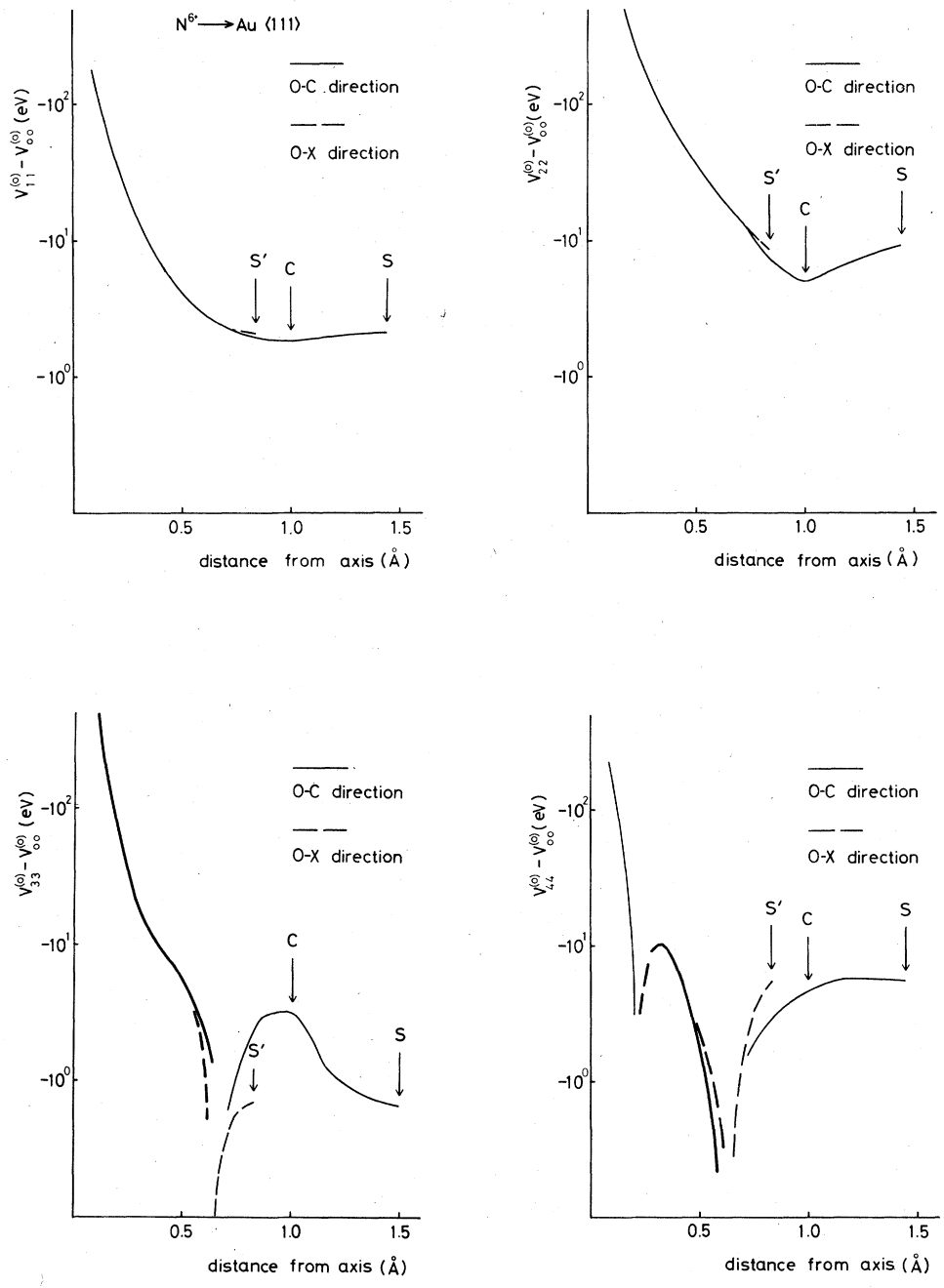

FIG. 5. Impact-parameter dependence of $V_{nn}^{(0)} - V_{00}^{(0)}$. The solid curve is for the direction O-C and the dashed for O-X in Fig. 4. The value of the bold line is positive.

the velocity of the Okorokov condition. The excitation profile for $0 \rightarrow 2$ is most modified from the symmetrical kinematic profile. On the other hand, the excitation profile for $0 \rightarrow 1$ is not so modified (except the peak position).

We show the total (averaged) ionization probabilities, $\langle |A_{\infty}|^2 \rangle_{\text{channel}}$, in Figs. 7–9 for $N^{6+} \rightarrow Au\ \langle 111 \rangle$. The upper right is the experimental curve by Moak *et al.*[1] By comparison, our theoretical profiles agree well with the experimental, especially the asymmetry of the profiles that are interpreted by our calculations. However, the profile for high index ($m = 6$)

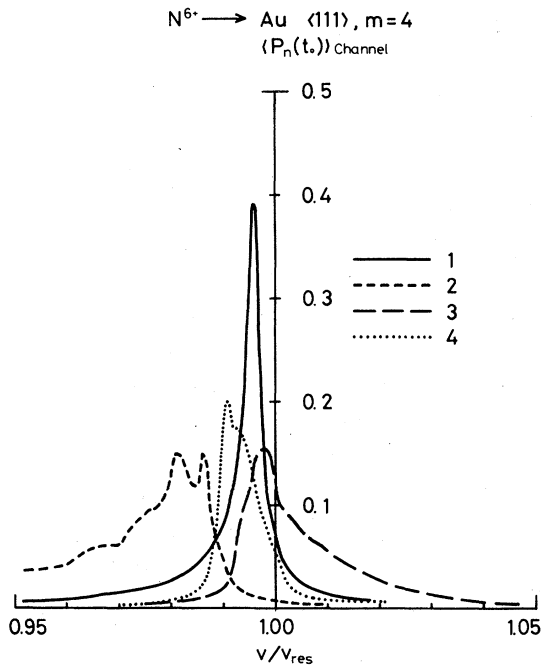

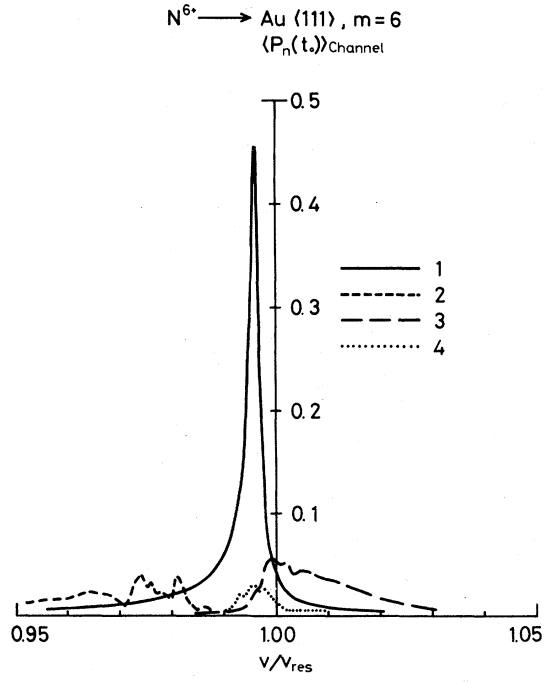

FIG. 6. The averaged excitation probabilities $\langle P_n \rangle_{\text{channel}}$ for each excitation level (1–4) for $N^{6+} \rightarrow$ Au ⟨111⟩ ($m = 4, 6$).

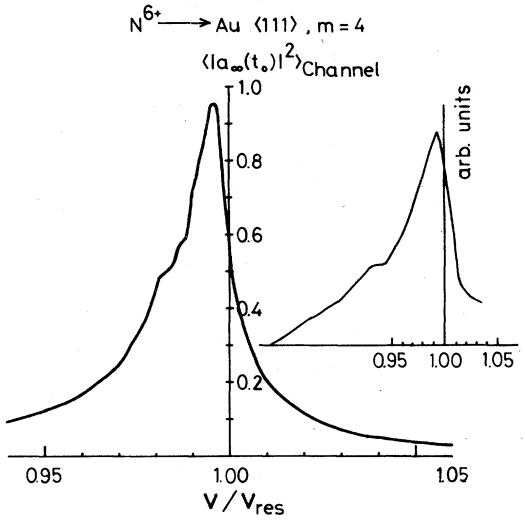

FIG. 7. Total (averaged) ionization probabilities $\langle |A_\infty|^2 \rangle_{\text{channel}}$ for $N^{6+} \rightarrow$ Au ⟨111⟩ ($m = 4$). The upper right is the experimental curve by Moak *et al.* (Ref. 1).

does not agree, which will be discussed in the next section.

VI. CONCLUDING REMARKS

By a dynamical theory, taking into account the ground state and the one excited state whose energy level splits into four states due to perturbation of the channeling wall atoms, we have calculated the detailed peak profile of the resonant coherent exciton of channeling ions. The peak profiles obtained here

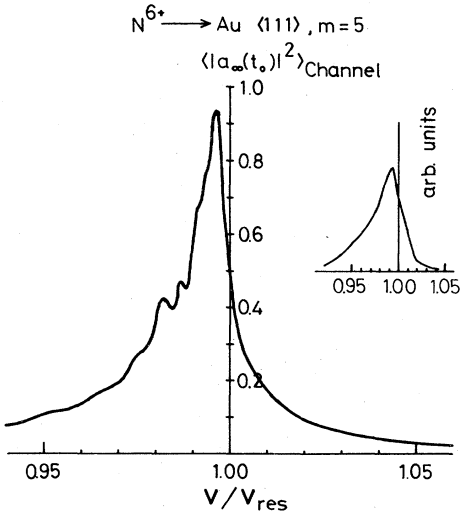

FIG. 8. Total (averaged) ionization probabilities $\langle |A_\infty|^2 \rangle_{\text{channel}}$ for $N^{6+} \rightarrow$ Au ⟨111⟩ ($m = 5$). The upper right is the experimental curve by Moak *et al.* (Ref. 1).

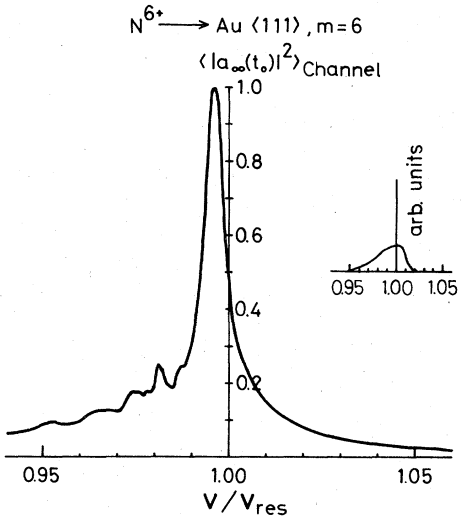

FIG. 9. Total (averaged) ionization probabilities $\langle |A_\infty|^2 \rangle_{\text{channel}}$ for $N^{6+} \rightarrow$ Au ⟨111⟩ ($m = 6$). The upper right is the experimental curve by Moak *et al.* (Ref. 1).

agree well with the experiments except for higher Miller indices.

The peaks for the higher Miller indices are sharper than the experimental ones. The temperature effect will contribute to a decrease in the peak height by the Debye-Waller factor. Table I shows the Debye-Waller factor $\exp(-2M_z)$ for various temperatures and the mirror indices, where M_z is defined by

$$M_z = \frac{1}{2}(2\pi m/d)^2 \langle u_z^2 \rangle \ ,$$

Where u_z is the thermal displacement of the atomic

TABLE I. Calculated Debye-Waller factors for various temperature and Miller indices.

Temperature (K)	$\exp(-2M_z)$ $m=4$	$\exp(-2M_z)$ $m=5$	$\exp(-2M_z)$ $m=6$
94	0.970	0.954	0.934
293	0.914	0.869	0.817
900	0.698	0.579	0.445

position in the channeling direction. It is noted that the Debye-Waller factor is only 0.817 for $m = 6$ and that the peak height decreases by 20%, which is not comparable to the experimental peak decrease. The energy loss or the stopping power may also modify our peak profile. However, it is not so easy to take into account the stopping power for the solution of Eq. (10).

Datz *et al.*[4] and Crawford and Ritchie[5] have pointed out the importance of the wake potential. They calculated the level splitting due to the wake potential for planar cases. However, in our calculation, we did not take into account the wake effect. In our case (axial channeling) the ion trajectories approach the atomic position more than the planar case and the splitting will be caused mainly by the lattice potential. However, the wake effect may also contribute to our calculation of the peak profile, which will be studied in the near future. It is noted also that the de-excitation process of ions while passing through the crystal prevents a coherent excitation profile.

[1]C. D. Moak, S. Datz, O. H. Crawford, H. F. Krause, P. F. Dittner, J. Gomez del Campo, J. A. Biggerstaff, P. O. Miller, P. Hvelplund, and H. Knudsen, Phys. Rev. A 19, 977 (1979).

[2]V. V. Okorokov, D. L. Tolchenkov, I. S. Khizhnyakov, Yu. N. Cheblukov, Y. Y. Lapitski, G. A. Iforov, and Yu. N. Zhukova, Phys. Lett. A 43, 485 (1973).

[3]S. Shindo and Y. H. Ohtsuki, Phys. Rev. B 14, 3929 (1976).

[4]S. Datz, C. D. Moak, O. H. Crawford, H. F. Krause, P. D. Miller, P. F. Dittner, J. Gomez del Campo, J. A. Biggerstaff, H. Knudsen, and P. Hvelplund (private communication).

[5]O. H. Crawford and R. H. Ritchie, Phys. Rev. A 20, 1848 (1979).